THE JOURNAL OF PHYSICAL CHEMISTRY B

ARTICLE

pubs.acs.org/JPCB

Kinetics of Micelle Formation and Concentration Fluctuations in Solutions of Short-Chain Surfactants

U. Kaatze*

Drittes Physikalisches Institut, Georg-August-Universität Göttingen, Friedrich-Hund-Platz 1, 37077 Göttingen, Germany

ABSTRACT: To study the kinetics of surfactant systems below, at, and above the critical micelle concentration cmc, broad-band ultrasonic spectra of short-chain ionic surfactant solutions are evaluated. Within the measurement frequency range from 100 kHz to 4.6 GHz the spectra reveal a relaxation term that, at variance with the classical theory of micelle formation, is subject to a broad distribution of relaxation times. Analysis of the shape of this term evidences a coupling between the kinetics of micelle formation/disintegration and noncritical fluctuations in the local concentrations of surfactant monomers, oligomers, and micellar structures. A theoretical model, based on the assumption of a rate process in parallel to the fluctuations, applies well to the broadness of the experimental spectra. An initial increase in the concentration dependence of the principle relaxation time above the cmc is compatible with the high content of oligomers but is more distinctive than predicted by an extended model of micelle formation. The dependence of the relaxation amplitude upon surfactant concentration indicates incomplete dissociation of counterions. An additional high-frequency wing in the spectra is assigned to different structure factors of monomers and micelles. It may, however, also contain contributions from relaxations due to the formation/disintegration kinetics of oligomers and to the structural isomerization of surfactant alkyl chains.

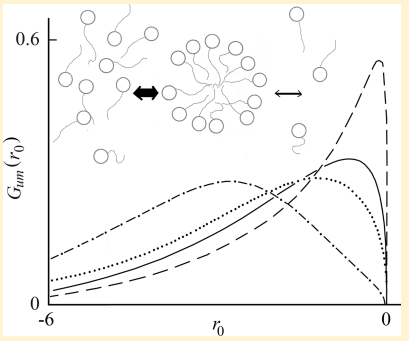

1. INTRODUCTION

Association of surfactants plays a significant role in the biosphere as well as in many technical processes. Proper micelle systems, both ionic and nonionic, are well conceived now.[1] Although it is not strictly defined, the term "proper systems" is used when solutions of globular micelles with mean aggregation numbers $\overline{m}$ on the order on or larger than 50 are considered. Globular micelles normally exist at surfactant concentration c sufficiently above the critical micelle concentration cmc and below the second cmc, at which larger aggregates, such as rod-like structures, are formed.[1,2] Typically, proper micelles from surfactants with alkyl chains of more than ten methyl groups, roughly corresponding with cmc values below 0.1 mol/L, have been studied. The micelle formation/disintegration kinetics can then be well represented by the Aniansson−Wall model[3−5] that proceeds from a stepwise association process, $N_{i-1} + N_1 \leftrightarrows N_i$, $i = 2, 3, ...$, with identical equilibrium constants $K_i = K_{\overline{m}}$ for all individual steps. Here N_i denotes an aggregate made of i monomers N_1. Additional constraints of the Aniansson−Wall model are a Gaussian size distribution of micelle sizes around the mean $\overline{m}$, small concentrations of oligomeric species, and a comparatively high concentration of monomers. The latter presumptions ensure irrelevance of micelle formation from (and disintegration into) two smaller aggregates and thus condition the above stepwise association of monomers.

Due to the small oligomer content the formation/disintegration kinetics of proper micelle systems is characterized by two characteristic time constants τ_f and τ_s. The smaller one, on the order of microseconds to milliseconds, refers to the fast exchange of monomers between micelles and the suspending phase. The larger one, with values typically between milliseconds and seconds, represents the relaxation, after a small disturbance, of the micelle size distribution to total equilibrium. As both the monomer exchange and the re-equilibration of micelle sizes involve changes in the molar volume of surfactant molecules, the associated relaxations can be sensitively disclosed by acoustical spectroscopy and its time-domain analogues, such as pressure-jump and temperature-jump techniques.[6] Theory[7,8] relates the relaxation amplitudes and relaxation times to the respective volume changes ΔV, assumed to be identical for all steps in the above reaction scheme, to the mean $\overline{m}$ of micelle sizes, to the variance σ^2 of the Gaussian distribution, and to the rate constant k_r $(=k^r_{\overline{m}})$ for micelle sizes at around the mean. Acoustical spectroscopy as well as related jump methods is therefore favorably used to determine these relevant parameters.

At surfactant concentrations near the cmc, however, Teubner−Kahlweit−Aniansson−Wall theory fails to predict the relaxation behavior due to monomer exchange correctly. With both ionic[9−13] and nonionic[14,15] micelle systems the dependence of the relaxation time upon surfactant concentration deviates characteristically from the theoretical predictions. Furthermore, instead of a discrete relaxation time, spectroscopy reveals a broad distribution of relaxation times.[12,16,17] This noteworthy feature has been assigned to the parallel action of micelle formation and disintegration processes as well as local fluctuations in concentration which, close to the cmc, likely act a perceivable influence

Received: June 8, 2011
Revised: July 11, 2011
Published: July 18, 2011

dx.doi.org/10.1021/jp205372g | J. Phys. Chem. B 2011, 115, 10470–10477

on the molecular dynamics. To understand the interference of concentration fluctuations with the micelle kinetics, it is thus interesting to study surfactant solutions below, at, and above the cmc. For this purpose acoustical spectra for aqueous solutions of a homologous series of *n*-alkylammonium chlorides are considered, including *n*-pentylammonium chloride with a cmc as high as about 1.9 mol/L. With such solutions fluctuations in the local concentration may predominate the micelle formation/disintegration processes. Hence at decreasing chain length within the homologous series of cationic surfactants a transition from almost proper micelle kinetics to predominantly fluctuation-controlled dynamics is expected. Acoustical spectroscopy is an adequate method as it has been widely used not just for the investigation of the micelle formation/disintegration kinetics of surfactant solutions but also for the study of critical[18] and noncritical concentration fluctuations[19−24] in mixtures.

2. EXPERIMENTAL SECTION

In this paper spectra from this laboratory for aqueous solutions of *n*-pentylammonium chloride (PeACl,[25] $CH_3(CH_2)_4NH_3^+Cl^-$) and *n*-hexylammonium chloride (HexACl,[26] $CH_3(CH_2)_5NH_3^+Cl^-$) are discussed and are compared to previous results for solutions of *n*-heptylammonium chloride (HepACl,[12] $CH_3(CH_2)_6NH_3^+Cl^-$) and *n*-octylammonium chloride (OcACl,[27] $CH_3(CH_2)_7NH_3^+Cl^-$). All surfactant solutions were prepared by adding appropriate amounts of hydrochloric acid solutions to preweighted quantities of the respective *n*-alkylamine, always tracing the pH potentiometrically. Deionized and additionally doubly distilled water was used to adjust the surfactant concentration of the measurement samples. The density ρ of the samples was determined with a pycnometer (20 mL, $\Delta\rho/\rho \leq 10^{-3}$, Schott, Mainz, Germany) that had been calibrated against doubly distilled and degassed water. Additional density measurements were performed with a vibrating-tube densitometer equipped with built-in reference oscillator and Peltier temperature control ($\Delta\rho/\rho \leq 5 \times 10^{-6}$, Physica DMA 5000, Anton Paar, Graz, Austria). The shear viscosity η_s of the solutions was measured with a falling ball viscometer (B/BH, Haake, Karlsruhe, Germany) and was checked by measurements with an Ubbelohde capillary viscometer (Schott, Germany). Temperature variations ΔT during the density and viscosity measurements were smaller than 0.02 K. The sound velocities c_s of the surfactant solutions were obtained as a byproduct from the ultrasonic absorption coefficient measurements described below. Data at 300 kHz were derived from the distance between resonance frequencies of cavity resonator cells.

The ultrasonic attenuation coefficient $\alpha(\nu)$ of the samples was measured as a function of frequency ν between 100 kHz and 4.6 GHz by applying two different methods. In the lower frequency range (0.1 MHz $\leq \nu \leq$ 23 MHz), where α is small, a cavity resonator method was appropriate in which multiple reflections virtually increased the pathway of interaction between the sample and the sonic field. At higher frequencies (3 MHz $\leq \nu \leq$ 4600 MHz) a pulse-modulated traveling wave method was employed in which the amplitude of the signal transmitted through the sample was determined as a function of liquid path length.

With all attenuation coefficient measurements the temperature *T* of the samples was controlled to within ±0.03 K and it was measured with an uncertainty of ±0.02 K. Temperature gradients within the specimen cells and temperature differences between different cells did not exceed 0.05 K, corresponding to an uncertainty $\Delta\alpha/\alpha < 0.001$. Fluctuations in the frequency of measurement were negligibly small throughout ($\Delta\nu/\nu <$ 0.0001). From repeated measurements and from the overlaps in the frequency ranges of data from different cells, the uncertainties in the attenuation coefficients were those given below: $\Delta\alpha/\alpha$ = 0.07, 0.1−0.8 MHz; $\Delta\alpha/\alpha$ = 0.04, 0.8−12 MHz; $\Delta\alpha/\alpha$ = 0.02, 12−60 MHz; $\Delta\alpha/\alpha$ = 0.01, 60−400 MHz; $\Delta\alpha/\alpha$ = 0.015, 400−530 MHz; $\Delta\alpha/\alpha$ = 0.01, 530−2000 MHz; $\Delta\alpha/\alpha$ = 0.03, 2000−4600 MHz.

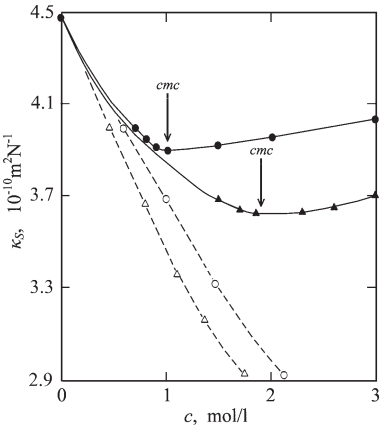

Figure 1. Adiabatic compressibility κ_s versus salt concentration *c* for aqueous solutions of PeACl (▲) and HexACl (●) as well as of tetraethylammonium (○) and tetrapropylammonium (Δ) bromide[28] at 25 °C. Arrows mark the cmc values as taken from the plots, respectively.

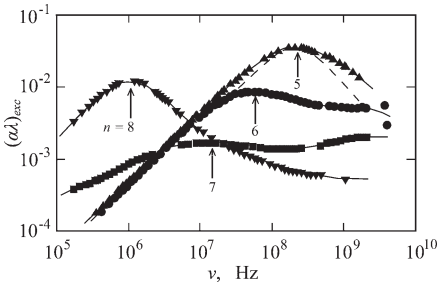

Figure 2. Ultrasonic excess attenuation per wavelength, $\alpha_{exc}\lambda$, at 25 °C displayed as a function of frequency, ν, for aqueous solutions of *n*-alkylammonium chlorides $CH_3(CH_2)_{n-1}NH_3^+Cl^-$) with surfactant concentration near the cmc (n = 5, c = 1.9 mol/L;[25] n = 6, c = 1 mol/L;[26] n = 7, c = 0.45 mol/L;[12] n = 8, c = 0.26 mol/L[27]). The dashed line represents a Debye-type relaxation spectral term with discrete relaxation time. Arrows indicate the relaxation frequency $(2\pi\tau)^{-1}$ of the low-frequency term in the spectra at different chain length *n*.

3. RESULTS

3.1. Critical Micelle Concentration. In Figure 1 the adiabatic compressibility κ_s, as according to the Newton−Laplace equation

$$\kappa_s = \rho^{-1} c_s^{-2} \quad (1)$$

calculated from the density ρ and sound velocity c_s, is shown as a function of surfactant concentration *c* for solutions of PeACl and HexACl and, for comparison, for solutions of two tetraalkylammonium salts. Whereas the κ_s data of the latter decrease

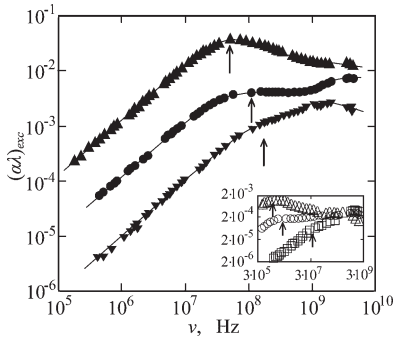

Figure 3. Ultrasonic excess attenuation spectra for aqueous solutions of HexACl (full symbols[26]) and OcACl (open symbols[27]) at different surfactant concentrations: ▼, c = 0.7 mol·L^{-1}; ●, c = 1 mol·L^{-1}; ▲, c = 1.5 mol·L^{-1}; □, c = 0.18 mol·L^{-1}; ○, c = 0.22 mol·L^{-1}; Δ, c = 0.24 mol·L^{-1}. Lines are graphs of relaxation spectral function $R_{H,D}(\nu)$ with parameter values as obtained by the regression analysis. Arrows show the relaxation frequency $(2\pi\hat{\tau})^{-1}$ of the low-frequency restricted Hill term.

monotonously with c, those for the short-chain surfactant systems display a relative minimum, indicating a transition region from solutions of molecularly dispersed surfactant to such with surfactant aggregates. Even though the transition region is rather broad, the minimum may be used to define critical micelle concentrations. The compressibility data suggest cmc = 1.9 mol/L for the PeACl system and cmc = 1 mol/L for the HexACl solutions which compares to cmc = 0.45 mol/L and 0.27 mol/L for HexACl and OcACl solutions, respectively. As will be shown below, these values are in fair agreement with indications from the ultrasonic attenuation spectra.

3.2. Ultrasonic Attenuation Spectra. Examples of ultrasonic attenuation spectra are shown in Figure 2 where, for solutions of the four cationic surfactants, the excess attenuation per wavelength

$$\alpha_{exc}\lambda = \alpha\lambda - B\nu \tag{2}$$

is displayed as a function of frequency ν. Here $\lambda = c_s/\nu$ is the wavelength of the sonic field and B is a parameter independent of ν. The B-term in eq 2 considers the asymptotic high-frequency contributions to the attenuation coefficient, which are predominantly due to Stokes' damping of sound because of viscous friction and which are of low interest here. The surfactant concentrations of the four solutions almost correspond with the cmc of the respective system.

Within the frequency range of measurement the spectrum of the PeACl system reveals one relative maximum, indicating one relaxation region. Obviously, the relaxation region extends over a significantly broader frequency range than a Debye-type relaxation term[29] with discrete relaxation time. Hence the underlying process is subject to a substantial distribution of relaxation times. With increasing number n of carbon atoms per alkyl chain of surfactant the relaxation frequency shifts downward, as marked in the figure by arrows. At the same time a wing appears in the spectra at frequencies above the relaxation region. Additional examples are presented in Figure 3 where spectra for HexACl solutions below, near and above the cmc are displayed as well as spectra for OcACl solutions at c < cmc. An eye-catching feature of these examples is the nonvanishing attenuation at concentrations well below the cmc.

3.3. Description of Spectra by Empirical Relaxation Function. A thorough inspection of the spectra shows that with PeACl solutions the relaxation time distribution is too broad to be represented by a sum of two Debye relaxation terms. Therefore, the restricted Hill function[30−32] ("H")

$$R_H(\nu) = \frac{A_H\omega\tau_H}{[1 + (\omega\tau_H)^{2s_H}]^{(1+n_H)/(2s_H)}} + B\nu \tag{3}$$

has been used[25] to analytically represent the measured total attenuation coefficient spectra. In this function A_H is an amplitude factor, τ_H is the principal relaxation time, parameters n_H and s_H control the width and shape of the underlying relaxation time distribution, and $\omega = 2\pi\nu$. To account for the high-frequency wing, spectra for solutions of HexACl and HepACl need an additional Debye ("D") relaxation term.[26,12] Hence

$$R_{H,D}(\nu) = \frac{A_H\omega\tau_H}{[1 + (\omega\tau_H)^{2s_H}]^{(1+n_H)/(2s_H)}} + \frac{A_D\omega\tau_D}{1 + \omega^2{\tau_D}^2} + B\nu \tag{4}$$

has been applied to empirically describe the experimental spectra. Here A_D is an amplitude and τ_D is the discrete relaxation time. Spectra of OcACl solutions reveal up to three relaxation regions. A sum of three Debye terms

$$R_{D,D,D}(\nu) = \sum_{i=1}^{3}\frac{A_{Di}\omega\tau_{Di}}{1 + \omega^2{\tau_{Di}}^2} + B\nu \tag{5}$$

has been found appropriate.[27]

Equations 3−5 have been fitted to the relevant experimental spectra using a nonlinear least-squares regression analysis[33] that causes the reduced variance

$$\chi^2 = \frac{1}{M-K-1}\sum_{m=1}^{M}\left(\frac{(\alpha\lambda)_m - R(\nu_m, P_k)}{(\Delta\alpha\lambda)_m}\right)^2 \tag{6}$$

to adopt its minimum. In this equation, ν_m, m = 1, ..., M, are the frequencies of measurements, $(\alpha\lambda)_m$ as well as $(\Delta\alpha\lambda)_m$ are the data and their experimental uncertainties, respectively, at these frequencies, R (=R_H, $R_{H,D}$, or $R_{D,D,D}$) is the relaxation function, and the P_k, k = 1, ..., K, are the parameters of R. The parameters obtained from the fitting procedure will be discussed in the following. In doing so, instead of τ_H and A_H, relaxation time $\hat{\tau} = (2\pi\hat{\nu})^{-1}$ and amplitude $\hat{A}$, corresponding with the frequency $\hat{\nu}$ at which the Hill term adopts its relative maximum, will be considered for comparability. These quantities relate to the Hill relaxation parameters as

$$\hat{\tau} = \tau_H n_H^{1/(2s_H)} \tag{7}$$

and

$$\hat{A} = 2A_H n_H^{-1/(2s_H)}(1 + 1/n_H)^{-(1+n_H)/(2s_H)} \tag{8}$$

4. DISCUSSION

4.1. Low-Frequency Term, Relaxation Time Distribution. The relaxation term of the PeACl spectra as well as the low-frequency term in the spectra of the other surfactant system evidently corresponds to the micelle formation/disintegration kinetics. With the OcACl solutions, which first of all may be considered proper micelle systems, the low-frequency term, in

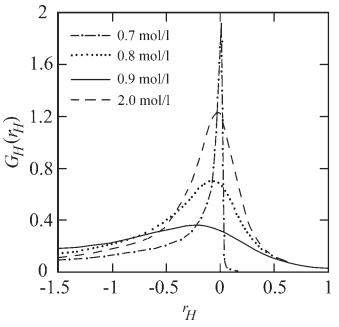

Figure 4. Relaxation time distribution function $G_H(r_H)$ of the restricted Hill term for HexACl aqueous solutions at four surfactant concentrations c.

conformity with theory,[7,8] can be well represented by a discrete relaxation time. According to our expectations the relaxation region broadens with decreasing length of alkyl chains, e.g., with increasing cmc and increasing variability in aggregate sizes. At four surfactant concentrations the relaxation time distribution function $G_H(r_H)$, $r_H = \ln(\tau/\tau_H)$, corresponding with the Hill relaxation spectral term of the HexACl system, is displayed in Figure 4. $G_H(r_H)$ is defined by the integral equation

$$R_H(\nu) = A_H \int_0^\infty G_H(r_H) \frac{\omega\tau}{1 + (\omega\tau)^2} \, dr_H \tag{9}$$

with

$$\int_{-\infty}^{\infty} G_H(r_H) \, dr_H = 1 \tag{10}$$

Here $G_H(r_H)$ has been calculated by analytical continuation[34]

$$G_H(r_H) = \frac{2\hat{G}}{\pi} \mathrm{Re}\left\{ \frac{-ie^{r_H}}{[1 + (-ie^{-r_H})^{2s_H}]^{(1+n_H)/(2s_H)}} \right\} \tag{11}$$

of the Hill spectral function, with $\hat{G}$ given by the normalization relation (eq 10).

In conformity with other short-chain surfactant solutions[12] the relaxation time distribution is rather narrow at $c <$ cmc, it becomes very broad at the cmc and it narrows again toward higher surfactant concentrations. Below the cmc the Hill term likely represents the formation/disintegration of premicellar oligomeric species. Approaching the cmc, two effects may contribute to a widening of the relaxation time distribution: establishment of a special distribution of aggregate sizes, causing the slow and fast processes in the Teubner–Kahlweit–Aniansson–Wall to convergence, and fluctuations in the local concentration of surfactant monomers and aggregates. Both effects will be addressed below. Above the cmc enhancement of the surfactant concentration results in an increasing content of micelles relative to oligomers and the system approaches more and more the predictions of the Teubner–Kahlweit model of proper micelle systems. Finally, the Hill term reflects the fast monomer exchange of the micelle formation/disintegration kinetics of proper micelle systems, as characterized by a discrete relaxation time.

4.2. Extended Model of Micelle Formation; Relaxation Time. To account for the broad relaxation time distribution of the Hill term, presumption of the size distribution as appropriate

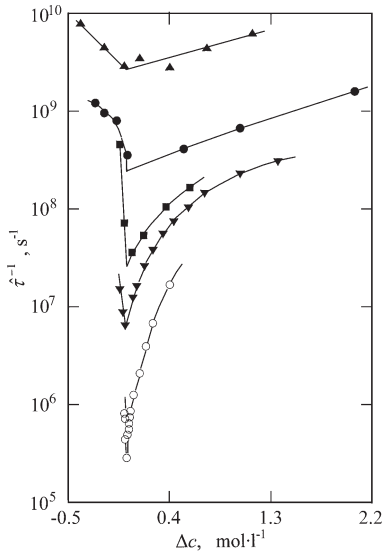

Figure 5. Relaxation rate $1/\hat{\tau}$, corresponding with the maximum in the restricted Hill term (eq 7), for some series of aqueous surfactant solutions at 25 °C displayed versus concentration difference $\Delta c = c$ − cmc: ▲, PeACl;[25] ●, HexACl;[26] ■, HepACl;[12] ▼, OACl;[27] ○, SDS.[13]

for proper micelle systems has been renounced.[35] Proceeding from the Teubner–Kahlweit theory,[7,8] reasonable relations for the forward (k_i^f) and backward ($k_i^b = k_i^f/K_i$) rate constants

$$k_{i+1}^f = k_{\bar{m}}^f (1 - s_f(i - \bar{m})) \tag{12}$$

$$k_{i+1}^b = k_{\bar{m}}^b (1 + s_b(i - \bar{m})) + k_2^b (1 + \exp[(1 - i_c)/d])/(1 + \exp[(i - i_c)/d]) \tag{13}$$

have been presumed instead of fixing the size distribution. In eqs 12 and 13 parameters $k(\frac{f}{\bar{m}})$ and $k(\frac{b}{\bar{m}})$ denote the forward and backward rate constant, respectively, at $i = \bar{m}$ and s_f and s_b control the point of intersection of the functions. They thus define $\bar{m}$. Parameters k_2^b, d, and i_c are related to the cmc and model the dependence of k_i^b upon i at small aggregation numbers. The linear behavior of functions $k_i^b(i)$ and $k_i^b(i)$ in the micelle regime guarantees a likewise Gaussian distribution of sizes in the micelle regime[36] with, as long as the concentration of monomers almost equals the cmc, its variance given by $\sigma^2 = (s_f + s_b)^{-1}$. Modeling the rate constants instead of assuming a fixed size distribution has the advantage to include nonproper micelle systems without sharp cmc. Another favorable feature of this extended Teubner–Kahlweit model is the fact that, in accordance with experimental evidence,[37,38] the mean aggregation number $\bar{m}$ as well as the variance σ^2, are allowed to vary with surfactant concentration c.

The extended model shows that, for systems with high cmc, the minimum located in the oligomer region of the size distribution is less distinctive, if not absent at all. Because of the flat minimum the fast and slow relaxations, featuring the formation/disintegration of proper micelle systems, converge. Convergence of the relaxation times τ_f and τ_s of the fast and slow process in the Teubner–Kahlweit theory when approaching the cmc may be one reason for the broadening of the relaxation time distribution in the ultrasonic spectra.

In addition, the extended model reveals an initial increase in the relaxation times with surfactant concentration at c close to

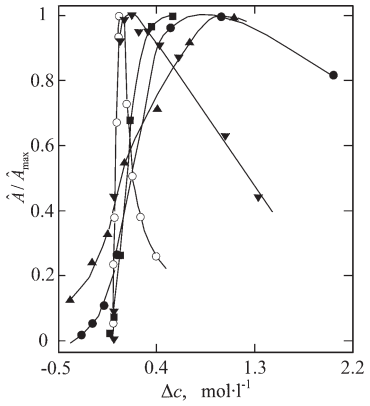

Figure 6. Normalized relaxation amplitude $\hat{A}$ (eq 8) of the restricted Hill term (eq 7) versus concentration difference $\Delta c = c -$ cmc for five series of ionic surfactant solutions at 25 °C: ▲, PeACl;[25] ●, HexACl;[26] ■, HepACl;[12] ▼, OACl;[27] ○, SDS.[13]

the cmc. As mentioned in the Introduction, experimental data are often at variance with the Teubner−Kahlweit−Aniansson−Wall model, which predicts ($\Delta c = c -$ cmc)

$$\tau_f = \frac{\sigma^2}{k_{\bar{m}}^b}\left(1 + \frac{\sigma^2}{\bar{m}}\frac{\Delta c}{\text{cmc}}\right)^{-1} \tag{14}$$

for the fast relaxation of proper micelle systems. Along with data for the prominent anionic surfactant sodium dodecylsulfate (SDS, $CH_3(CH_2)_{11}SO_4^-Na^+$), relaxation rates $\hat{\tau}^{-1}$ of the Hill term in the ultrasonic spectra for solutions of the homologous series PeACl, HexACl, HepACl, and OACl are displayed in Figure 5. With each system the relaxation rates adopt a clear minimum at the respective cmc. Simulation of the extended Teubner−Kahlweit model has evidenced the trend in the relaxation rate data. The minimum, however, appeared to be less distinct than featured by the experimental data.

Another noticeable characteristic of the relaxation rates is the significant dependence of the minimum values $\hat{\tau}_{min} = \hat{\tau}^{-1}(\text{cmc})$ upon the length of surfactant alkyl chain ($\hat{\tau}_{min} = 2.8 \times 10^5$ s^{-1}, SDS; $\hat{\tau}_{min} = 2.4 \times 10^9$ s^{-1}, PeACl), exposing a considerable slowing in the micelle formation/disintegration processes at increasing molecular volume.

4.3. Micelle Formation and Incomplete Dissociation of Counter Ions; Relaxation Amplitude. If data are available at sufficiently high solute concentrations the amplitudes $\hat{A}$ of the ionic surfactant systems, including SDS, display a pronounced relative maximum (Figure 6). This behavior can be consistently explained by the assumption of incomplete counterion dissociation of micellar aggregates.[39] This assumption means a coupling between the counterion dissociation/association equilibrium to the coupled scheme of micelle formation/disintegration which leads to a concentration dependence in the monomer concentration. Hence $\bar{N}_1 = \bar{N}_1(c)$ instead of $\bar{N}_1 =$ cmc. Consequently, in the theory of micelle formation $\Delta c/$cmc should be replaced by the reduced concentration $X = (c - \bar{N}_1(c))/\bar{N}_1(c)$. The expressions for the relaxation time (eq 14) as well as the relaxation amplitude relation then read

$$\tau_f = \frac{\sigma^2}{k_{\bar{m}}^b}\left(1 + \frac{\sigma^2}{\bar{m}}\frac{c - \bar{N}_1(c)}{\bar{N}_1}\right)^{-1} \tag{15}$$

and

$$A_f = \frac{\pi(\Delta V)^2}{\kappa_S^\infty RT}\frac{\sigma^2}{\bar{m}}\frac{c - \bar{N}_1(c)}{\bar{N}_1}\left(1 + \frac{\sigma^2}{\bar{m}}\frac{c - \bar{N}_1(c)}{\bar{N}_1}\right)^{-1} \tag{16}$$

respectively. According to the law of mass action

$$\frac{\bar{N}_i}{\bar{N}_{i-1}\bar{N}_1\bar{N}_c^{(J_i - J_{i-1})}} = b_i \tag{17}$$

the monomer concentration $\bar{N}_1$ is related to the concentration $\bar{N}_i$ of class i micellar species and the concentration $\bar{N}_c$ of free counterions. Here $J_i = i(1 - \alpha_i)$ denotes the number of nondissociated monomers per class i aggregate, α_i is the effective degree of counterion dissociation, and b_i is the equilibrium constant of step i. Only for proper micelle systems α_i may be assumed independent of i ($\alpha_i = \alpha_{\bar{m}}$) and the aggregation number may be sufficiently large to replace $\bar{m} - 1$ by $\bar{m}$. On these presumptions, the monomer concentration follows from the implicit relation

$$\bar{N}_1 = (\sqrt{2\pi}\sigma\bar{m}b_{\bar{m}})^{1/\bar{m}(2-\alpha_{\bar{m}})}\left(\frac{c}{\bar{N}_1} - 1\right)^{1/\bar{m}(2-\alpha_{\bar{m}})} \times \left[1 + \alpha_{\bar{m}}\left(\frac{c}{\bar{N}_1} - 1\right)\right]^{(1-\alpha_{\bar{m}})/(2-\alpha_{\bar{m}})} \tag{18}$$

Using this relation along with the reasonable value $\alpha_{\bar{m}} = 0.33$[40] and with estimates $\bar{m} = 11$, 17, 20, and 25 for the cationic surfactants CH_3CH_{n-1} $NH_3^+Cl^-$ with $n = 5$, 6, 7, and 8, backward rate constants 16×10^9, 8×10^9, 2×10^9, and 0.8×10^9 s^{-1}, respectively, have been derived[25] from the slope $d\hat{\tau}^{-1}/dX = k_{\bar{m}}^b/\bar{m}$ in the relaxation rates (eq 15). In these calculations σ values between 6.7 (PeACl) and 18 (OcACl) have been used in eq 18. Correspondingly, reaction volumes ΔV between 4 cm^3·mol^{-1} (PeACl) and 6.5 cm^3·mol^{-1} (OcACl) followed from the relaxation amplitudes $\hat{A}$.[25]

The above $k_{\bar{m}}^b$ and the ΔV values display a reasonable dependence upon alkyl chain length. The distinct increase in the backward rate constant with n clearly reflects the stronger bonding of monomers with longer alkyl chain in the micellar structures. The increase in the reaction volume reveals the enhanced effect of hydrophobic hydration around monomers with longer chains and the thus larger change in the water density when the surfactant exchanges between an aggregate and the suspending phase.

4.4. Noncritical Concentration Fluctuations. Although the trends in the parameters related to the micelle formation/disintegration kinetics support an isodesmic reaction scheme, the extended Teubner−Kahlweit−Aniansson−Wall model does not quantitatively account for two features of the ultrasonic spectra of short-chain surfactants. First, it does not disclose the tremendous broadness of the relaxation time distribution of the spectra at concentrations near the cmc (Figure 4) and, second, it only partly represents the initial decrease with surfactant concentration in the relaxation rate below the cmc (Figure 5). For that reason the experimental spectra have been alternatively

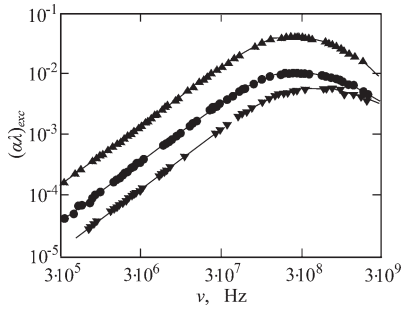

Figure 7. Ultrasonic excess absorption spectra for three PeACl solutions in water at 25 °C:[25] ▼, c = 1.5 mol·L^{-1}; ●, c = 1.7 mol·L^{-1}; ▲, c = 2 mol·L^{-1}. Lines show relaxation spectral function $R_{um}(\nu)$ with parameter values from the fitting procedure.

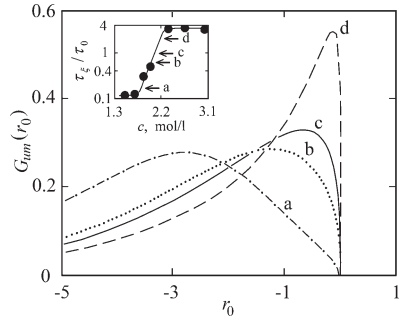

Figure 8. Relaxation time ratio τ_ξ/τ_0 of the unifying model of concentration fluctuations versus surfactant concentration c (inset) and relaxation time distribution function $G_{um}(r_0)$ at four τ_ξ/τ_0 values (eqs 25 and 26), as marked by arrows in the inset.

analyzed in terms of spectral function

$$R_{um}(\nu) = Q\int_0^\infty \frac{q^2}{w(q)}\frac{\omega\tau_g}{1+\omega^2{\tau_g}^2}\,dq \qquad (19)$$

of the unifying model ("um") of noncritical concentration fluctuations.[24] Combining relevant features of previous theoretical models of noncritical concentration fluctuations,[19−23] this model proceeds from the idea that local differences in the concentration may equalize by diffusion and in parallel by a rate process. In eq 19 Q is an amplitude and the weight function

$$w(q) = [1 + 0.164(q\xi) + 0.25(q\xi)^2]^{-2} \qquad (20)$$

has been chosen to model long-range correlations ($r > \xi$) by the usually considered Ornstein−Zernike behavior and short-range correlations ($r < \xi$) by a nearly exponential decay.[21] Parameter ξ is the characteristic length in the spatial correlation of concentration fluctuations. Hence it reflects the average size of the rapidly changing fluctuations.

The spectral function (eq 19) has been derived assuming differential equation

$$\partial\phi(\vec{r},t)/\partial t = (D\nabla^2 - 1/\tau_0)\phi(\vec{r},t) \qquad (21)$$

to control the time behavior in the autocorrelation function $\phi(\vec{r},t)$ of a suitable order parameter which at $\vec{r}$ and t represents the deviation of the local concentration from the mean. Here D is the mutual diffusion coefficient which according to the

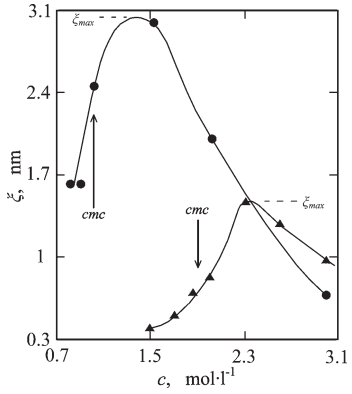

Figure 9. Fluctuation correlation length ξ versus surfactant concentration c for solutions of PeACl[25] and HexACl[26] in water at 25 °C.

Kawasaki−Ferrell relation[41,42]

$$D = \frac{k_B T}{6\pi\eta_s\xi} \qquad (22)$$

is related to the correlation length ξ. Quantity k_B denotes Boltzmann's constant. Parameter τ_0 is the relaxation time of the rate process, such as a dimerization or a conformational variation. Relaxation time τ_g in eq 19 is defined as

$${\tau_g}^{-1} = Dq^2 + {\tau_0}^{-1} \qquad (23)$$

Even though $R_{um}(\nu)$ contains only the three unknown parameters (Q, D, τ_0) it fits well to the broad low-frequency term in the measured spectra. Some examples exposing the nice agreement of the theoretical function and the experimental data are displayed in Figure 7, where spectra of the PeACl system are shown for which no interference with additional relaxation terms exists.

In Figure 8 relaxation time τ_0 of the rate process in the PeACl solutions is compared to the relaxation time

$$\tau_\xi = \xi^2/(2D) \qquad (24)$$

which, in correspondence with the dynamic scaling hypothesis,[43] is assumed to control the decay by diffusion of fluctuations with average size ξ. Association of surfactant molecules around the cmc is reflected by a distinct increase in the τ_ξ/τ_0 ratios of the PeACl system with c. With the HexACl and HepACl solutions the behavior of the τ_ξ/τ_0 values is not as significant, likely because of interference with the additional high-frequency Debye-type relaxation term in the spectra.

Also shown in Figure 8 at some τ_ξ/τ_0 ratios is the relaxation time distribution function $G_{um}(r_0)$ which, by analogy to eq 9, conforms to $R_{um}(\nu)$. If $r_0 = \ln(\tau/\tau_0)$

$$G_{um}(r_0) = 0 \quad \text{at} \quad r_0 > 0 \qquad (25)$$

and

$$G_{um}(r_0) = \hat{G}_{um}\frac{[e^{r_0}(1-e^{r_0})]^{1/2}}{[e^{r_0} + 0.328\{(\tau_\xi/\tau_0)e^{r_0}(1-e^{r_0})\}^{1/2} + (\tau_\xi/\tau_0)(1-e^{r_0})]^2} \qquad (26)$$

otherwise. Below the cmc the relaxation time distribution of the PeACl solutions is very broad, as characteristic for diffusive processes. Approaching the cmc, $G_{um}(r_0)$ appears to be already markedly cut at $r_0 = 0$. Fluctuations with relaxation times τ_ξ larger

than τ_0 are short-circuited by the formation of oligomeric and micellar structures. The cutoff in the relaxation time distribution is clearly visible at the cmc, where $\tau_{\bar{\xi}} \approx \tau_0$ (curve c, Figure 8), and it is even more distinctive at concentrations above the cmc, where at $\tau_{\bar{\xi}} > \tau_0$, the dynamics is dominated by the aggregate formation/disintegration processes even though fluctuations in the local concentration still exist.

For two short-chain surfactant systems the fluctuation correlation lengths $\bar{\xi}$, according to the Kawasaki−Ferrell relation (eq 22) calculated from the diffusion coefficients D and shear viscosities η_s, are displayed as a function of surfactant concentration c in Figure 9. With both series of data the $\bar{\xi}$ values first increase to reach a maximum at $c \approx$ cmc + 0.4 mol/L. Toward even higher concentrations, namely at increasing content of complete micelles, the fluctuation correlation length decreases. The finding of the maximum correlation length $\bar{\xi}_{max}$, and thus maximum relaxation times $\tau_{\bar{\xi}max}$ (eq 24), to increase with the length of surfactant alkyl chain corresponds with a similar trend in the data of aqueous solutions of nonaggregating molecules, such as alcohols, alkoxyalkanols, and derivatives of urea.[24] It supports the idea that alkyl groups of the nonaqueous constituent substantially promote fluctuations in the local concentration.[24]

Quite remarkably the unifying model applies excellently to the experimental spectra of PeACl, HexACl, and HepACl solutions, even though it considers the aggregate formation/disintegration by only one rate process instead of by the complete scheme of coupled reactions. The low-frequency Debye-type relaxation term in the spectra of OcACl solutions corresponds well[27] with the monomer exchange process in the Aniansson−Wall−Teubner−Kahlweit model[7,8] of proper micelle systems for which a discrete relaxation time is predicted.

4.5. High-Frequency Wing. In addition to the low-frequency relaxation term, high-frequency contributions exist in the ultrasonic spectra that can be represented by one (PeACl, HexACl, HepACl) or two (OcACl) Debye relaxations. With the HexACl system the relaxation times (0.023 ns $\leq \tau_D \leq$ 0.094 ns) of this relaxation are even shorter than with HepACl solutions (0.08 ns $\leq \tau_D \leq$ 0.16 ns[12]). Taking into account that τ_D will further decrease at decreasing length of alkyl chains, a Debye term likely exists also with the PeACl solutions but is located well above our frequency range of measurement ($\nu \leq$ 4.6 GHz). These high frequency contributions may reflect several features of surfactant solutions, as will be briefly discussed below.

A recent theoretical approach, based on a Kubo formalism,[44,45] of the ultrasonic attenuation of nonionic surfactant systems revealed flat high frequency contributions to the spectra[17] as resulting from different structure factors $S_1(q)$ and $S_{\bar{m}}(q)$ of monomers ("1") and micelles ("$\bar{m}$"). Neglecting for simplicity the size distribution of micelles all aggregates have been characterized by only one species with aggregation number $\bar{m}$. Ornstein−Zernike behavior, corresponding with correlation

$$S_1(r) = (\hat{S}_1/r)\exp(-r/\bar{\xi}_1) \tag{27}$$

has been assumed for monomers and, postulating a faster structure factor falloff at large r,

$$S_{\bar{m}}(r) = (\hat{S}_{\bar{m}}/r^2)\exp(-r/\bar{\xi}_{\bar{m}}) \tag{28}$$

has been presumed for aggregates. Here $\hat{S}_1$ and $\hat{S}_{\bar{m}}$ are amplitudes and $\bar{\xi}_1$ as well as $\bar{\xi}_{\bar{m}}$ are correlation lengths. With the notations $D_{eff} = D_1 + D_{\bar{m}}$ and $\tau_{eff}^{-1}\,\tau_1^{-1} + \tau_{\bar{m}}^{-1}$ for the effective diffusion coefficient and relaxation time, respectively, the relaxation spectral function for the ternary system reads

$$R_t(\nu) = \hat{R}_t \int_0^\infty \frac{\omega\, \mathrm{d}^3 q \qquad D_{eff}q^2 + \tau_{eff}^{-1}}{(q^2 + \bar{\xi}_1^{-2})(q^2 + \bar{\xi}_{\bar{m}}^{-2})^{1/2}(D_{eff}q^2 + \tau_{eff}^{-1})^2 + \omega^2} \tag{29}$$

with amplitude factor $\hat{R}_t$. Independent of whether $\bar{\xi}_{\bar{m}} \ll \bar{\xi}_1$ or $\bar{\xi}_{\bar{m}} \gg \bar{\xi}_1$ this function displays high-frequency contributions because in the former case, with $\omega^* = \omega(\bar{\xi}_{\bar{m}}^2/D_{eff})$,

$$R_t(\nu) \propto 1 - (2/(\pi\omega^*))\ln\omega^* \tag{30}$$

and in the latter

$$R_t(\nu) \propto 1 - (2/\pi)(\omega^* \ln\omega^* + \pi/2)/(1 + \omega^{*2}) \tag{31}$$

In addition to contributions from the different structure factors of monomers and aggregates, other mechanism may add to the high-frequency part of the spectra. Further, to the merging of the slow and fast relaxation processes, the extended Teubner−Kahlweit model of the micelle formation reveals an ultrafast relaxation process due to the monomer exchange of oligomers.[35] The Debye term in the spectra of HexACl and HepACl solutions as well as one high-frequency term of the OcACl/water spectra may thus, at least in part, also reflect the oligomer kinetics. Another molecular process that seems to contribute to ultrasonic spectra of micelle solutions is the structural isomerization of the alkyl chains within the micellar core. The relaxation time of the structural isomerization of normal alkanes decreases from 0.29 ns for *n*-hexadecane to 0.08 ns for *n*-decane.[46] Hence likely the high-frequency Debye terms in the spectra of HexACl ($\tau_D \approx$ 0.05 ns), HepACl ($\tau_D \approx$ 0.12 ns), and OcACl ($\tau_D \approx$ 0.4 ns) solutions contain contributions from chain isomerization. This assumption is supported by the fact that, within a rather narrow frequency range (relaxation times between 0.15 and 0.29 ns[27]), hypersonic relaxation terms have been found for several anionic, cationic, and nonionic surfactant solutions. Independency of the relaxation times from the nature of the surfactant head groups suggests a relaxation process related to the micellar cores.

5. CONCLUSIONS

Broad-band ultrasonic attenuation spectra (0.1 $\leq \nu \leq$ 4600 MHz) of aqueous solutions of short-chain *n*-alkylammonium chlorides reveal a relaxation term related to the micelle (and oligomer) formation/disintegration kinetics. Octylammonium chloride solutions behave like a proper micelle system in that the relaxation term reveals a discrete relaxation time as, within the framework of the Teubner−Kahlweit−Aniansson−Wall model,[7,8] predicted for the monomer exchange. The relaxation term broadens significantly when going to shorter alkyl chains. A particularly broad distribution of relaxation times emerges at surfactant concentrations near the respective cmc. This feature has been taken to indicate the micelle kinetics to be noticeably affected by fluctuations in the local concentrations of surfactant monomers and aggregates. Analytically, the broad relaxation term can be well described by a theoretical model in which concentration fluctuations are assumed to occur in parallel to a rate process. At surfactant concentrations below the cmc the

molecular dynamics is dominated by diffusion. Approaching the critical micelle concentration, more and more oligomers and small micellar structures are formed. In addition to diffusion aggregate formation/disintegration comes to the fore, cutting the relaxation time distribution at large values. Finally, at surfactant concentrations distinctly above the cmc, the dynamics is increasingly controlled by the formation/disintegration kinetics. As diffusion of fluctuations plays a minor role, the relaxation time distribution narrows and the system approximates the behavior of proper micelle solutions. Despite the agreement between theory and experiment, the former suffers from the fact that one rate process is considered only instead of the complete isodesmic scheme of reactions, which is normally implied.

With each surfactant the micelle formation/disintegration term of the spectra reveals principal relaxation times that first increase with surfactant concentration c to decrease with c above the cmc. This finding can, at least qualitatively, be explained by an extended version of the Teubner−Kahlweit−Aniansson−Wall theory in which the attempt is made to model size distribution in the oligomer region more realistically.[35] According to our expectation, such a version predicts a high content of oligomers in the concentration range near the cmc, involving a faster monomer exchange. A noteworthy dependence of the maximum relaxation time at the respective cmc upon the length of surfactant alkyl chain reflects the effect of molecular volume in the monomer exchange kinetics.

The amplitude of this term does not monotonously increase with c to asymptotically reach a maximum value but decreases with c at concentrations well above the cmc. Such concentration dependence in the relaxation amplitude is well explained by inclusion of the effect from incomplete dissociation of counterions of ionic surfactants.[39]

A high-frequency wing in the attenuation spectra of surfactant solutions except PeACl had been already found with many ionic and nonionic micelle solutions. It may simply be partly due to the fact that different structure factors are relevant for the monomers and the surfactant aggregates.[17] Fast oligomer formation may also contribute to the high-frequency part of the spectra. In addition, as an ultrasonic relaxation term with corresponding relaxation time is also characteristic for liquid n-alkanes[46] at room temperature, structural isomerization of the surfactant alkyl chains within the micellar cores likely is also reflected by the sonic excess attenuation within that frequency range.

AUTHOR INFORMATION

Corresponding Author

*Tel.: +49 551 39 7715. Fax: +49 551 39 7720. E-mail address: uka@physik3.gwdg.de.

REFERENCES

(1) Evans, D. F.; Wennerström, H. *The Colloidal Domain. Where Physics, Chemistry, and Biology Meet*; Wiley-VCH: New York, 1999.
(2) Haller, J.; Kaatze, U. *J. Phys. Chem. B* **2009**, *113*, 12283–12292.
(3) Aniansson, E. A. G.; Wall, S. N. *J. Phys. Chem.* **1974**, *78*, 1024–1030.
(4) Aniansson, E. A. G.; Wall, S. N. *J. Phys. Chem.* **1975**, *79*, 857–858.
(5) Aniansson, E. A. G. *Prog. Colloid Polym. Sci.* **1985**, *70*, 2–5.
(6) Strehlow, H. *Rapid Reactions in Solution*; VCH: Weinheim, 1992.
(7) Teubner, M. *J. Phys. Chem.* **1979**, *83*, 2917–2920.
(8) Kahlweit, M.; Teubner, M. *Adv. Colloid Interface Sci.* **1980**, *13*, 1–64.
(9) Adair, D. A. W.; Reinsborough, V. C.; Trenholm, H. M.; Valleau, J. P. *Can. J. Chem.* **1976**, *54*, 1162–1167.
(10) Hall, D. G.; Wyn-Jones, E. *J. Mol. Liq.* **1986**, *30*, 63–83.
(11) Frindi, M.; Michels, B.; Levy, H.; Zana, R. *Langmuir* **1994**, *10*, 1140–1145.
(12) Telgmann, T.; Kaatze, U. *J. Phys. Chem. B* **1997**, *101*, 7758–7765.
(13) Polacek, R.; Kaatze, U. *J. Phys. Chem. B* **2007**, *111*, 1625–1631.
(14) Frindi, M.; Michels, B.; Zana, R. *J. Phys. Chem.* **1994**, *98*, 6607–6611.
(15) Telgmann, T.; Kaatze, U. *J. Phys. Chem. A* **2000**, *104*, 1085–1094.
(16) Telgmann, T.; Kaatze, U. *Langmuir* **2002**, *18*, 3068–3075.
(17) Bhattacharjee, J. K.; Kaatze, U. *J. Phys. Chem. B* **2011**, *115*, 6069–6075.
(18) Bhattacharjee, J. K.; Kaatze, U.; Mirzaev, S. Z. *Rev. Prog. Phys* **2010**, *73*, 066601 (36 pp).
(19) Romanov, V. P.; Solov'ev, V. A. *Sov. Phys. Acoust.* **1995**, *11*, 68–71.
(20) Romanov, V. P.; Solov'ev, V. A. *Sov. Phys. Acoust.* **1995**, *11*, 219–220.
(21) Montrose, C. J.; Litovitz, T. A. *J. Acoust. Soc. Am.* **1970**, *47*, 1250–1257.
(22) Endo, H. *J. Chem. Phys.* **1990**, *92*, 1986–1993.
(23) Romanov, V. P.; Ul'yanov, S. V. *Phys. A* **1993**, *201*, 527–542.
(24) Rupprecht, A.; Kaatze, U. *J. Phys. Chem. A* **1999**, *103*, 6485–6491.
(25) Polacek, R. *Dissertation*, Georg-August-University, Göttingen, 2003.
(26) Hagen, R. *Diploma-Thesis*, Georg-August-University, Göttingen, 1998.
(27) Polacek, R.; Kaatze, U. *J. Mol. Liq.* **2010**, *157*, 125–132.
(28) Kühnel, V.; Kaatze, U. *J. Phys. Chem.* **1996**, *100*, 19747–19757.
(29) Debye, P. *Polare Molekeln*; Hirzel: Leipzig, 1929.
(30) Hill, R. N. *Nature* **1978**, *275*, 96–99.
(31) Hill, R. N. *Phys. Status Solidi* **1981**, *103*, 319–328.
(32) Menzel, M.; Rupprecht, A.; Kaatze, U. *J. Acoust. Soc. Am.* **1998**, *104*, 2741–2749.
(33) Marquardt, W. M. *J. Soc. Ind. Appl. Math.* **1963**, *11*, 431–441.
(34) Giese, K. *Adv. Mol. Relax. Processes* **1973**, *5*, 363–373.
(35) Telgmann, T.; Kaatze, U. *J. Phys. Chem. B* **1997**, *101*, 7766–7772.
(36) Aniansson, E. A. G. *Ber. Bunsen-Ges. Phys. Chem.* **1978**, *82*, 981–988.
(37) Chan, S. K.; Herrmann, U.; Ostner, W; Kahlweit, M. *Ber. Bunsen-Ges. Phys. Chem.* **1977**, *81*, 60–66.
(38) Chan, S. K.; Herrmann, U.; Ostner, W; Kahlweit, M. *Ber. Bunsen-Ges. Phys. Chem.* **1977**, *81*, 396–402.
(39) Lessner, E.; Teubner, M.; Kahlweit, M. *J. Phys. Chem.* **1981**, *85*, 1529–1536.
(40) Adair, D. A. W.; Hicks, J. R.; Jobe, D. J.; Reinsborough, V. C. *Aust. J. Chem.* **1983**, *36*, 1021–1025.
(41) Kawasaki, K. *Phys. Rev. A* **1970**, *1*, 17501757.
(42) Ferrell, R. A. *Phys. Rev. Lett.* **1970**, *24*, 11691172.
(43) Anisimov, M. A. *Critical Phenomena in Liquids and Liquid Crystals*; Gordon and Breach: Philadelphia, 1991.
(44) Kubo, R. *J. Phys. Soc. Jpn.* **1957**, *12*, 570586.
(45) Kubo, R.; Toda, M.; Hashitsune, N. *Statistical Physics II*, 2nd ed.; Springer: Berlin, 1991.
(46) Behrends, R.; Kaatze, U. *J. Phys. Chem. A* **2000**, *104*, 3269–3275.